Supplementary Information

New materials for infrared non linear optics. Syntheses, structural characterisations, second harmonic generation and optical transparency of $M(IO_3)_3$ metallic iodates.

Phanon Delphine, Mosset Alain, Gautier-Luneau Isabelle*

Laboratoire de Cristallographie, CNRS, associé à l'Université Joseph Fourier, 25 avenue des Martyrs, BP 166, 38042 Grenoble Cedex 9, France

Table S1 Selected interatomic distances (Å) (with e.s.d) and bond angles (°) (with e.s.d) for α-$In(IO_3)_3$ and β-$In(IO_3)_3$.

α-$In(IO_3)_3$		β-$In(IO_3)_3$	
In-O1	2.136(4) x3	In-O1	2.156(3) x3
In- O3^{I}	2.139(5) x3	In- O3^{I}	2.141(3) x3
I-O1	1.827(4)	I-O1	1.825(3)
I-O2	1.778(5)	I-O2	1.803(4)
I-O3	1.833(5)	I-O3	1.798(3)
I- O1^{V}	3.014(5)	I- O2^{V}	2.567(4)
I- O2^{III}	2.696(5)	I- O2^{III}	3.024(4)
I- O3^{I}	2.915(5)	I- O1^{VI}	3.115(4)
O1-In- O1^{II}	88.7(2)	O1^{IV}-In-O1	84.9(1)
O1-In- O3^{I}	84.5(2)	O1-In- O3^{I}	89.8(1)
O1-In- O3^{III}	96.1(2)	O1-In- O3^{II}	174.7(1)
O1-In- O3^{IV}	171.6(2)	O1-In- O3^{III}	94.0(1)
O3^{I} -In- O3^{III}	91.3(2)	O3^{I}-In- O3^{II}	91.2(1)
O1-I-O2	97.9(2)	O2-I-O1	99.7(2)
O1-I-O3	95.1(2)	O2-I-O3	101.4(2)
O2-I-O3	100.6(2)	O1-I-O3	96.5(2)

Symmetry card for α-$In(IO_3)_3$: ^{I} (1-x, 1-y, z+1/2); ^{II} (1–x+y, 1-x, z); ^{III} (y, -x+y, z+1/2); ^{IV} (x-y+1, x, z+1/2); ^{V} (x-y, x, z+1/2).
Symmetry card for β-$In(IO_3)_3$: ^{I} (1/3-x, 2/3-y, 5/3-z) ; ^{II} (y-2/3, -x+y-1/3, 5/3-z) ; ^{III} (x-y+1/3, x-1/3, 5/3-z) ; ^{IV} (-x+y, -x, z) ; ^{V} (y+1/3, 2/3-x+y, 5/3-z) ; ^{VI} (2/3-x, 1/3-y, 4/3-z).

Phase transition of of α-$In(IO_3)_3$ in β-$In(IO_3)_3$

In order to determine the transition temperature, temperature dependent X-ray powder diffraction experiments have been performed. X-ray powder diffraction patterns of α-$In(IO_3)_3$ and β-$In(IO_3)_3$ are presented in Fig. S1. The evolution of the powder patterns has been followed on the most intense peaks in the range 26° to 43° (Fig. S2). This experiment shows the transformation of α-$In(IO_3)_3$ to β-$In(IO_3)_3$ at around 365°C. The phase transition is not reversible.

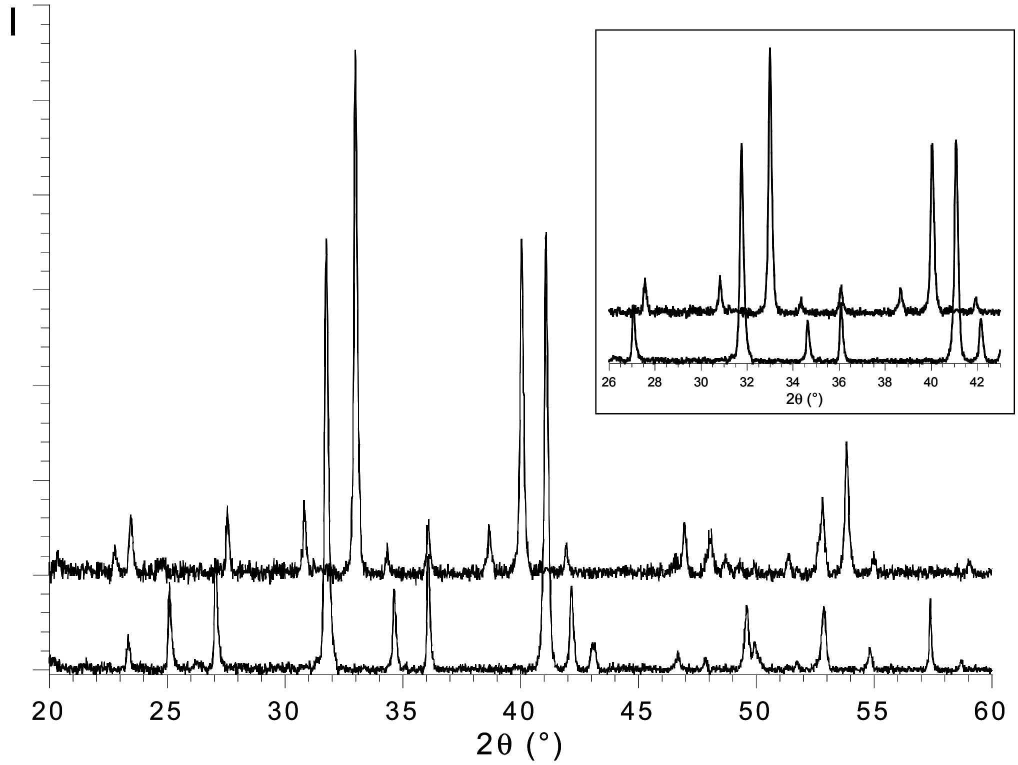

Fig. S1 X-ray diffraction powder patterns of *α*-$In(IO_3)_3$ (bottom) and *β*-$In(IO_3)_3$ (top) recorded at $\lambda(Fe_{\alpha1})$ = 1.93604 Å. The insert shows the powder patterns of the most intense peaks in the range 26° to 43°.

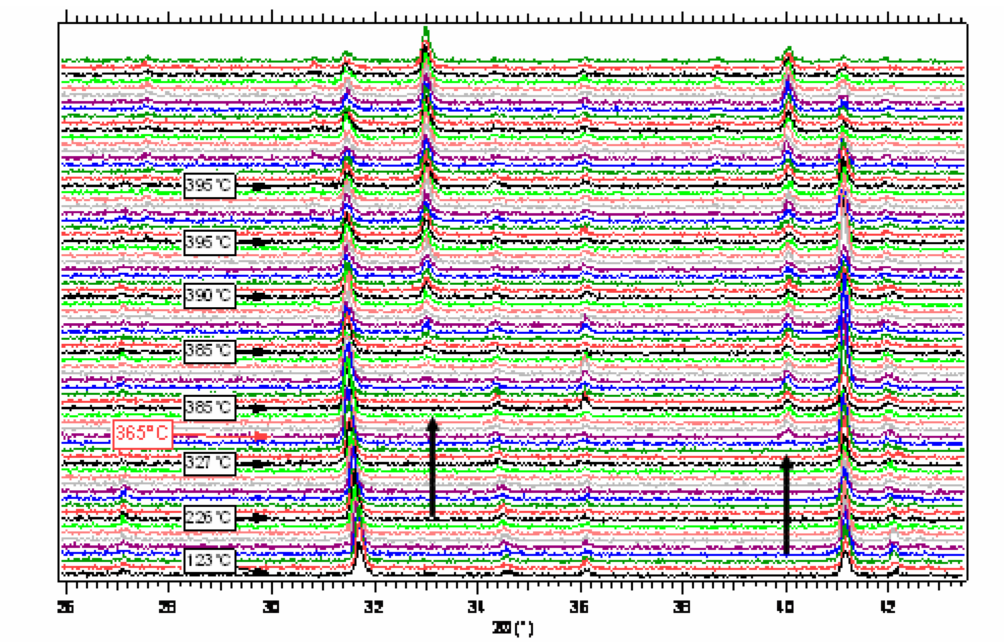

Fig. S2 Temperature dependent powder diffraction patterns of *α*-$In(IO_3)_3$ (2θ range 26° to 43°). Arrows indicate the apparition of peaks of the *β*-$In(IO_3)_3$ phase.

DSC analyses: DSC analyses for compounds α-In(IO_3)$_3$, β-In(IO_3)$_3$ and Ga(IO_3)$_3$ were carried out on a NETZSCH ATD-DSC 404S apparatus and ran in the range 25-600°C, in argon flow at 5°C/min heating rate (Fig. 10).

For α-In(IO_3)$_3$, the DSC curve shows decomposition at 535°C which corresponds to the formation of indium oxide In_2O_3 (JCPDS file no. 71-2194). However, α-In(IO_3)$_3$ undergoes a phase transition at about 365°C which isn't observed on the DSC curve. The DSC curve of β-In(IO_3)$_3$ shows the same thermal behaviour as α-In(IO_3)$_3$. So, for clarity, it was not represented in Fig. 10.

For Ga(IO_3)$_3$, it reveals decomposition at around 525°C. The composition of the residue was determined by X-ray powder diffraction and identified as being the gallium oxide γ-Ga_2O_3 (JCPDS file no. 20-0426).

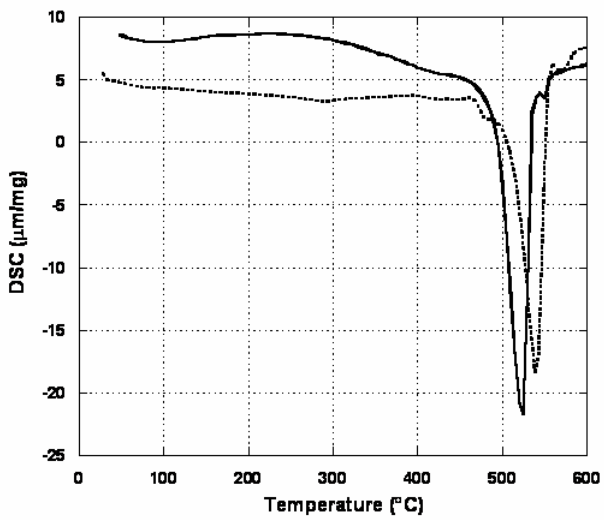

Fig. S3 DSC curves of Ga(IO_3)$_3$ (black line) and α-In(IO_3)$_3$ (dotted line).